



HAL
open science

Gold nanoparticles supported onto amine-functionalized in-capillary monoliths meant for flow-through catalysis: A comparative study

Romain Poupart, Mohamed Guerrouache, Daniel Grande, Benjamin Le Droumaguet, Benjamin Carbonnier

► To cite this version:

Romain Poupart, Mohamed Guerrouache, Daniel Grande, Benjamin Le Droumaguet, Benjamin Carbonnier. Gold nanoparticles supported onto amine-functionalized in-capillary monoliths meant for flow-through catalysis: A comparative study. *Polymer*, 2021, 230, pp.124014. 10.1016/j.polymer.2021.124014 . hal-03306860

HAL Id: hal-03306860

<https://hal.science/hal-03306860>

Submitted on 29 Jul 2021

HAL is a multi-disciplinary open access archive for the deposit and dissemination of scientific research documents, whether they are published or not. The documents may come from teaching and research institutions in France or abroad, or from public or private research centers.

L'archive ouverte pluridisciplinaire **HAL**, est destinée au dépôt et à la diffusion de documents scientifiques de niveau recherche, publiés ou non, émanant des établissements d'enseignement et de recherche français ou étrangers, des laboratoires publics ou privés.

Gold Nanoparticles Supported onto Amine-Functionalized In-Capillary Monoliths Meant for Flow-Through Catalysis: A Comparative Study

Romain Poupart, Mohamed Guerrouache, Daniel Grande, Benjamin Le Droumaguet* and Benjamin Carbonnier*

Univ Paris Est Creteil, CNRS, ICMPE, UMR 7182, 2 rue Henri Dunant, 94320 Thiais, France.

* Corresponding author: Benjamin Le Droumaguet, Benjamin Carbonnier,

Tel : +33 (0)1 49 78 11 77.

Fax: +33 (0)1 49 78 12 08.

E-mail address: ledroumaguet@icmpe.cnrs.fr, carbonnier@icmpe.cnrs.fr

Keywords: Gold nanoparticles, Catalytic reduction, Monolith, Amino-functionalization, Polymer-supported nano-metal

Abstract:

Monoliths functionalized with ethylene diamine-derived ligands were synthesized within micro-sized channels as highly permeable catalytic supports for the immobilization of *in-situ* generated gold nanoparticles. The as-obtained hybrids, essentially differing on the grafted amine containing ligands were compared, notably regarding the immobilized nanoparticles morphology and their dispersion at the monolith pore surface. Further, such in-capillary hybrid monoliths were successfully applied as flow-through microreactors for the catalytic reduction of nitroaromatic compounds. The general synthetic route for preparing these composite materials consisted in a three-step procedure involving (i) UV-induced polymerization of *N*-acryloxysuccinimide and ethylene glycol dimethacrylate in toluene, (ii) surface grafting of a series of ethylene diamine derivatives through nucleophilic substitution of *N*-hydroxysuccinimide leaving groups, and (iii) successive *in situ* reduction of tetrachloroauric acid to generate monolith-adsorbed gold nanoparticles. The successful synthesis of such hybrid monoliths was ascertained by *in-situ* Raman spectroscopy, EDX analysis and SEM observations. Microscopy demonstrated the key role of the grafted amine bearing ligand regarding the morphology, size and surface coverage of the immobilized gold nanoparticles at the monolith pore surface. Monolith-adsorbed gold nanoparticles exhibited good catalytic activities towards the conversion of nitroaromatic compounds into the corresponding amino derivatives in a flow-through process. This study clearly demonstrates the key role of the nature, primary vs. secondary, of the chelating amine in the morphology (shape, size, dispersion) of the supported gold nanoparticles.

1. Introduction

Miniaturization in materials chemistry had led to the development and the improvement of various strategies and methods to design and tailor performant microreactors. Among this type of reactors, polymer-based systems have emerged to be very promising for flow-through catalytic processes. [1-5] The properties of the continuous interconnected porous polymer matrix, also called monolith, which can be easily prepared by polymerization of various commercially available styrenic or (meth)acrylic monomers, can be tuned by grafting of ligands so as to change the interfacial features of the polymeric surface. [6] For instance, the polymer matrix can be functionalized with different chemical groups (*e.g.* amine, thiol, cyano or carboxylic acid among them) that notably allow for the grafting of several metallic nanoparticles. Svec *et al.* [7] pioneered the use of such cross-linked polymers as monolithic stationary phases for electrochromatographic and chromatographic applications. [8] Since then, the technology has evolved and has been broadened to a plethora of solutes (hydrophobic, hydrophilic, ionic and chiral) that can be now efficiently separated.

On the other hand, metallic nanoparticles are well-known as supported nano-catalysts for various organic reactions: dye reduction, [9] nitro compound reduction [10-11] or C-C cross-coupling such as Heck, [12-13] Sonogashira [14] or Suzuki-Miyaura [15] reactions. Noble metal-based nanoparticles relying on platinum, [13] palladium [10, 16] or silver [17] have been the subject of numerous studies. However, gold is so far the most commonly used noble metal for polymer-based heterogeneous catalyzed reactions. [18] One of the major advantages of such monolith-immobilized metallic nanoparticle relies on the facile supported catalyst recovery and the easy reusability of the hybrid systems. Over the last years, a large variety of such nanoparticles@polymer hybrids has been prepared in our laboratory to implement such heterogeneous supported catalytic reactions. Some of us notably demonstrated that catalytic nanoreactors could be obtained upon immobilization of gold nanoparticles at the pore surface of oriented nanoporous polystyrene originating from diblock copolymers possessing a selectively cleavable junction. [19-20] It was notably demonstrated that cascade reactions could be envisioned with some of those systems to carry out more complex chemical processes, leading eventually to higher added value molecular transformations. [20] Some bulk monoliths have also been prepared from selectively cleavable disulfide containing dimethacrylate crosslinker. [21] These monoliths could be consecutively modified by chemical reduction of the disulfide bond, affording some available thiol groups at the pore surface of the polymer, further used to immobilize nanogold, thus

allowing for a pollutant dye, *i.e.* Eosin Y, reduction. Different hybrid monolithic systems based on biporous polymeric materials have also been prepared from a functionalizable monomer, *i.e.* HEMA. [22] Finally, a plethora of examples, in which monoliths are covalently linked to the inner wall of ~ 100 μm -diameter fused silica capillaries, has been reported in our group. All these in-capillary monoliths relied on a functionalizable monomer that can be modified by a post-polymerization reaction with a chemical graft of interest to allow for further nanometal immobilization. These systems were not only assessed for their flow-through supported catalysis abilities but also for their separation behaviour. In this context, GCMA- [2] but more importantly NAS-based [1, 3, 23] polymers have been investigated in different works.

Studies on nanometals immobilized at the pore surface of polymers generally focus on the ability of different chemical function (*e.g.* thiol, amine, *etc*) to chelate metallic ions. [24-26] Some comparisons were notably achieved regarding the impact of the nature of the chemical function at the pore surface towards metallic nanoparticle immobilization. [27] Simultaneously, other efforts have been made to fully understand the nucleation and growth processes of the gold nanoparticles in colloidal solution [28-29] or onto a substrate. Athanassiou research group has reported a lot on the preparation of nanoparticles through the impregnation of chitosan with gold, [30] silver, [31] palladium [32] and platinum [32] salt precursors and the subsequent reduction into their respective nanoparticles through a laser-mediated UV irradiation. Another alternative strategy relies on the reductive properties of the support, such as polystyrene [9] or silicone [33-34] to generate gold nanoparticles. Finally, thermal annealing after impregnation of the polymer with a metal salt precursor has also been reported to be successfully implemented for the preparation of metallic nanoparticles. [35] As demonstrated from these studies, the *in situ* strategy allows for the preparation of a large variety of size- and density-controlled metal nanoparticles within desired areas of polymeric supports. However, no investigation regarding the shape of the metal ligand has been developed so far. In this context, we decided to investigate the effect of amine-derived ligand chemical structure at the pore surface of polymeric monolithic columns on the chelation of gold nanoparticles. Thus, ethylene diamine derivatives are prone to chelate a wide variety of metal ions.

Hence, in the present work, we investigate the crucial role of chelating groups anchored at the monolith surface, notably in terms of gold nanoparticle morphology, dispersion, and homogeneity. Specifically, ethylenediamine (EDA), tetraethylenepentamine (TETRA), 1-(2-aminoethyl)piperazine (AEP), and tris(2-aminoethyl)amine (TRIS) were used

as ligands of choice while *in-situ* generated gold nanoparticles are immobilized onto the amine-functionalized monolith *via* reduction of HAuCl_4 with sodium borohydride (NaBH_4). The as-obtained monoliths are finely characterized, notably by scanning electron microscopy (SEM) and Energy-dispersive X-ray spectroscopy (EDX). Finally, these hybrid monoliths are successfully applied to the flow-through reduction of nitro-compounds in the presence of NaBH_4 . This work enables the establishment of relationships between the nature of the ligand and the features of the immobilized gold nanoparticles.

2. Experimental

2.1. Materials

N-Acryloxysuccinimide (NAS, $\geq 98\%$) and toluene ($>99.5\%$) were obtained from TCI. 3-(Trimethoxysilyl)propyl methacrylate (γ -MAPS, 98%), sodium borohydride (NaBH_4 , 98%), sodium hydroxide (NaOH , 0.1 M), hydrochloric acid (HCl , 0.1 M for HPCE), ethylenediamine (EDA, $\geq 99.8\%$), tris(2-aminoethyl)amine (TRIS, 96%), tetraethylenepentamine (TETRA, 98%), 1-(2-aminoethyl)piperazine (AEP, 99%), and 4-nitroaniline (*p*-nitroaniline, $\geq 99\%$) were purchased from Sigma Aldrich. Ethylene glycol dimethacrylate (EGDMA, 98%) and 2,2'-azobisisobutyronitrile (AIBN, 98%) were obtained from Acros Organics. 2-Nitrophenol (*o*-nitrophenol, 98%), and 4-chloro-7-nitrobenzofurazan (99%) were purchased from Alfa Aesar. Acetone, and HPLC grade acetonitrile (ACN) were supplied by Carlo Erba. All reagents were used without any further purification, except from AIBN that was recrystallized from MeOH and stored at 4 °C prior to use. 18.2 M Ω deionized water was filtered through a Milli-Q Plus purification pack. Fused silica capillaries with a UV-transparent external coating (100 μm I.D.) were obtained from Polymicro Technologies.

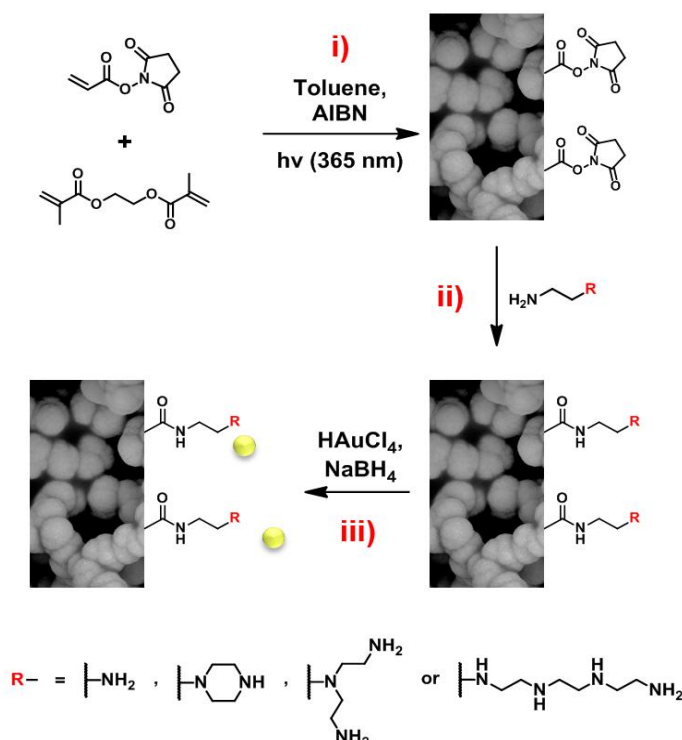
2.2. Instrumentation

An HPLC pump (Shimadzu LC-10ATVP) was used to flush monolithic columns with nitroarenes solutions. Spectrolinker XL-1500 UV Crosslinker (Spectronics Corporation) equipped with six lamps ($6 \times 15\text{W}$, 365 nm) was used to photoinitiate monomer copolymerization. UV-Vis spectra were recorded on a Cary 60 UV-Vis Spectrophotometer from Agilent Technologies. The chemical structure of monoliths was investigated using a Raman apparatus XPlora One from Horiba Jobin Yvon equipped with a laser emitting at 638 nm. Samples were investigated in different places of the cross sections to control the

homogeneity of monoliths. The acquisition time was fixed at 1 min. Scanning Electron Microscopy (SEM) investigation of the materials was performed with a MERLIN microscope from Zeiss equipped with InLens, EBSD, and SE2 detectors using a low accelerating tension (2-3 kV) with a diaphragm aperture of 30 μm . Prior to analyses, the samples were coated with a 4-nm layer of palladium/platinum alloy in a Cressington 208 HR sputter-coater. Energy-dispersive X-ray spectroscopy (EDX) was performed using a SSD X-Max detector of 50 mm^2 from Oxford Instruments (127 eV for the $\text{K}\alpha$ ray of Mn). (Hybrid) Monolithic capillary columns were cut at different places and small pieces were deposited on a SEM support with double-face adhesive tape. For the EDX analyses, the size of the investigated area was changed and the presented data were obtained for the analysis of 1 μm^2 representing nearly the size of a polymeric globule and represent averaged values obtained measurements performed at 5 different locations from three samples (Table S1). It was notably observed that similar results were observed independently of the probed area. The size of the Au NP was estimated using ImageJ software (Table S2).

2.3. Synthesis of in-capillary monoliths

The synthesis of the monolithic columns relied on a two-step process involving (i) the synthesis of the macroporous acrylate-based matrix and (ii) the surface chemical modification of the matrix with one of the amine ligands, as shown in **Scheme 1**.



Scheme 1. Schematic representation of the synthetic route applied to the design and synthesis of Poly(NAS-*co*-EGDMA) monoliths grafted with different ethylene diamine derivatives for the immobilization of *in-situ* generated gold nanoparticles: i) Poly(NAS-*co*-EGDMA)

monolith synthesis, *ii*) functionalization of Poly(NAS-*co*-EGDMA) with amine containing ligands, and *iii*) immobilization of gold nanoparticles at the pore surface of amine functionalized Poly(NAS-*co*-EGDMA) monoliths *via* the *in-situ* strategy.

2.3.1. Surface pre-treatment of capillaries

In order to ensure the stability of the monolithic column, the inner wall of the capillaries was submitted to a vinylization step. 3-(Trimethoxysilyl)propyl methacrylate was used as a bifunctional reagent allowing for the covalent attachment of the polymeric material onto the inner wall of the capillaries. The procedure was as follows: fused silica capillaries were treated with 1.0 M NaOH for 1h at room temperature and subsequently heated for 2 h at a temperature of 100 °C. Capillaries were flushed with 0.1 M HCl for 10 min, rinsed with deionized water for 10 min, and then with acetone for 15 min. Thereafter, capillaries were purged with dry nitrogen gas for 2 h at a temperature of 120 °C. A 30 vol.% 3-(trimethoxysilyl)propyl methacrylate solution in toluene was allowed to react overnight with inner silanols at room temperature. Last, the capillaries were rinsed with toluene for 15 min and dried under a stream of nitrogen gas for 1 h. The capillaries thus treated were stored at 4 °C.

2.3.2. *In-situ* synthesis of porous monolith

The porous monolith was prepared through a polymerization reaction of a mixture consisting of the following combination: NAS as a functional monomer, EGDMA as a crosslinker, toluene as a porogenic solvent, and AIBN as an initiator (1 wt.% with respect to the total amount of monomers). The mixture was sonicated for about 15 min to obtain 15 min to obtain homogeneous solution. The pre-treated capillary was completely filled with the polymerization mixture by immersing the inlet of the capillary into a reservoir and by pushing through the solution under nitrogen pressure (3 bar). After flushing with a large excess of polymerization solution, both ends of the capillary were sealed with rubber septa and the capillary was placed within a Spectrolinker XL-1500 UV and irradiated during 800s. After the polymerization was completed, the septa were removed and the monolith capillary was washed with ACN for 1 h ($5 \mu\text{L}\cdot\text{min}^{-1}$) to remove the porogenic solvent.

2.3.3. *In-situ* functionalization of the porous monolith with amine ligands

The succinimide groups stemming from the NAS moieties were replaced into different amine groups through nucleophilic substitution reaction. The reaction was performed *in-situ*

by flushing the monolith capillary with a solution of EDA, TRIS or AEP (0.3 M \approx 100 μ L in 2 mL of ACN in a reservoir) or TETRA (0.3 M = 200 μ L in 2 mL of ACN in a reservoir) pushed under nitrogen pressure (50 bar) during 3 h at room temperature. Thereafter, the monolithic capillary was washed with ACN for 1 h to remove unreacted ligands. The completion of nucleophilic substitution was evaluated through *in-situ* Raman spectroscopy performed on monolithic capillary samples.

2.3.4. Formation of *in situ* gold nanoparticles (AuNPs)

The amine-modified monolith was primarily flushed with an HCl solution during 15 min to protonate the amine function into quaternary ammonium. Then, it was flushed with a 1 wt. % HAuCl₄ solution in deionized water until all the capillary was totally coloured in yellow. It was then rinsed with deionized water during 1 h to remove the un-grafted gold ions. Then, a solution of NaBH₄ (10 mL, 0.1 M) in deionized water was flushed during 2 h. Finally, the capillary was flushed with deionized water for 30 min. A change in the colour appearance of the capillaries was observed as they turned to dark purple suggesting the effective formation of Au⁰.

2.3.5. Reduction of nitroarenes by supported heterogeneous catalysis

A freshly prepared solution containing 200 μ L of nitroarenes (*i.e.* 5 mg of *o*-nitrophenol, 4-chloro-7-nitrobenzofurazan or *p*-nitroaniline in 10 mL H₂O), 200 μ L of NaBH₄ (114 mg in 10 mL H₂O) in 5 mL of water was injected in the loop of a HPLC pump system, the solution coming out from the in-capillary AuNP-decorated monoliths was collected and then analysed by UV-Vis spectrophotometry. This catalytic flow reactions were performed at a flow rate of 3 μ L.min⁻¹ and gold-free monoliths substituted with the amine ligands were used as control monoliths.

3. Results and Discussion

3.1. Functionalization of in-capillary polymer monoliths

Svec research group reported the preparation of poly(glycidyl methacrylate-*co*-ethylene glycol dimethacrylate)-based monoliths that were successively chemically modified with thiol functions.[24-25] Such sulfhydryl functions were used to tightly immobilize gold nanoparticles. Alternatively, our group took advantage of the amine functions of both cysteamine and ethylene diamine to anchor gold nanoparticles at the pore surface of *N*-acryloxysuccinimide-based monolithic columns.[36] On top of that, Liu *et al.* recently used

another imidazole containing ligand, *i.e.* histamine, to the same purpose. Site-specific immobilization of commercially available preformed gold nanoparticles was achieved upon straightforward dynamic loading of the functionalized monolithic capillary with a gold colloidal solution.[37] Other strategies to efficiently anchor gold nanoparticles onto porous materials relied on their preparation through an *in-situ* process involving percolation of a chloroauric acid solution as a AuNP precursor and subsequent reduction of metallic ions with sodium borohydride [21] or *via* the Turkevitch method[38] involving citrate.[39] A two-step process was necessary for preparing amine-bearing porous monoliths within fused silica capillaries (inner diameter of 100 μm), as shown in **Scheme 1**. After activation of the inner wall of the capillary in the presence of γ -MAPS, a functional reactive acrylic monomer, *i.e.* *N*-acryloxysuccinimide (NAS), and EGDMA as a cross-linking agent were copolymerized in the presence of AIBN (1 wt.% with respect to the total amount of co-monomers) and toluene as a radical initiator and a porogenic solvent, respectively. Upon filling the pre-activated capillary with this polymerization mixture, sealing of the extremities with rubber septa and subsequent photo-initiated copolymerization within a UV oven at 365 nm, an in-capillary Poly(NAS-*co*-EGDMA) monolith was obtained with nucleophile-sensitive *N*-hydroxysuccinimide activated ester functionality and well-defined interconnected pores in the micrometer-sized range, as reported in previously published results in the field.[23, 40-45]

A post-polymerization modification was then investigated on the as-obtained Poly(NAS-*co*-EGDMA) monolith so as to functionalize the *N*-hydroxysuccinimide functions with nucleophilic amine derivatives from ethylene diamine (Figure S1). Four different derivatives were assessed, namely ethylene diamine (EDA), tris(2-aminoethyl)amine (TRIS), tetraethylenepentamine (TETRA), and 1-(2-aminoethyl)piperazine (AEP). Flushing of the different amine bearing ligands through the monolithic capillary allowed for a total consumption of the *N*-hydroxysuccinimide activated ester moieties of the monolith. This was ascertained by *in-situ* Raman spectroscopy of the in-capillary monoliths before and after post-polymerization modification that pointed out the complete disappearance of characteristic bands of succinimidyl esters present in the pristine poly(NAS-*co*-EDMA) at 1730 (imide asymmetric stretching), 1780 (imide symmetric stretching) and 1810 cm^{-1} (activated ester stretching) corresponding to the carbonyl stretching modes, as already published elsewhere.[40-45, and see Figures S4-6] Additionally, the occurrence of bands assigned to amide bonds (at 1300 cm^{-1} , 1550 cm^{-1} and 1650 cm^{-1}), as shown in **Figure 1**, confirmed the covalent attachment of the four different ethylene diamine-based ligands at the monolith surface through amide bond coupling.[23] Finally, a band assigned to the $-\text{NH}$ stretching

mode was observed at 3300 cm^{-1} in all the amine-functionalized Poly(NAS-*co*-EGDMA) in-capillary monoliths. This clearly demonstrated the efficiency of the grafting onto the functional reactive NHS functionalities by a straightforward nucleophilic substitution.

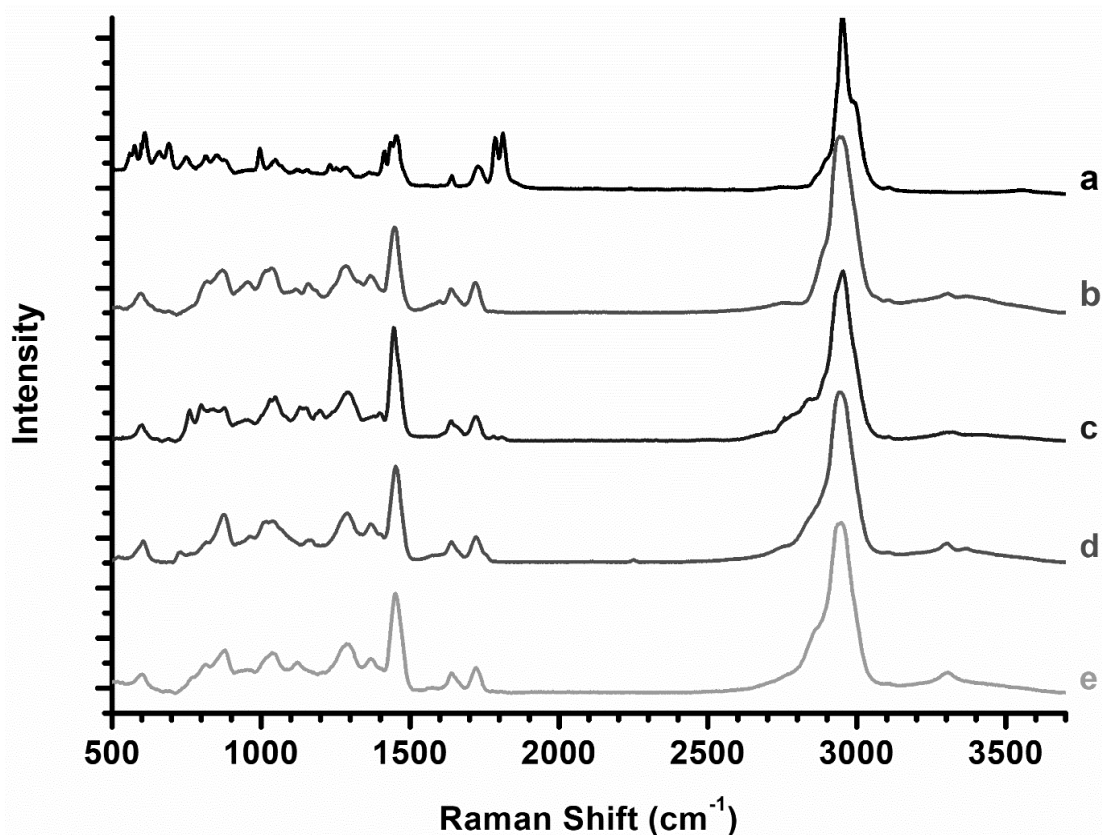


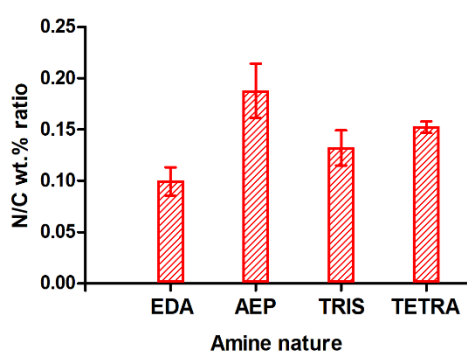
Figure 1. Raman spectra of Poly(NAS-*co*-EGDMA)-based monoliths a) before or after functionalization with b) EDA, c) AEP, d) TRIS or e) TETRA ligands.

3.2. *In-situ* formation of AuNPs

Immobilization of AuNPs onto porous polymers has been well-described in the literature in the last decades, notably by taking advantage of the chemical functions exhibited at the pore surface, including thiol-, [37, 46] cyano-, [46] and amine [1, 20] functions, to cite but a few. Surprisingly, even if some investigations on the crucial role of the chemical function on the AuNPs adsorption has been reported (thiol *vs.* amine for instance), [37] no comparative study has hitherto been investigated on the influence of ligands over AuNPs adsorption. To fill this gap, we thus focused on the effect of different ethylenediamine-based ligands on the shape, morphology, dispersion and coverage density of *in-situ* generated AuNPs over such amine functionalized Poly(NAS-*co*-EGDMA)-based monolithic capillaries. The adsorption of AuNPs was achieved through a two-step *in-situ* strategy. First, chloroauric acid solution (HAuCl_4) was percolated through the polymeric monolith. Then, the hydride-mediated reduction of Au^{3+} cations was achieved by flowing a NaBH_4 solution through the capillary

and allowed for the preparation of hybrid AuNPs@polymeric monoliths. Semi-quantitative EDX analyses of the different resulting amine-functionalized hybrid monolithic capillaries were realized to investigate the surface composition of the porous monoliths after grafting of the amine ligands and in situ synthesis of the gold nanoparticles. Thereby, the prominent features in the EDX patterns are assigned to the characteristic chemical signals of carbon, nitrogen, oxygen and gold (Figure S2). Such profiles are in full agreement with the Raman data and confirm not only the successful grafting of the amine ligands but also the presence of gold at the surface of the functionalized monoliths. To gain further information about the surface composition of the hybrid monoliths, the nitrogen over carbon and gold over nitrogen atomic ratios were calculated for the four types of ligands (Figure 2 and Table S1). The highest N/C value was obtained for the monolith functionalized with 1-(2-aminoethyl)piperazine (0.19) that is nearly twice the lowest value obtained for the ethylene diamine functionalized monolith (0.1). Rather similar N/C ratio values (~ 0.14) were obtained for the monoliths functionalized with tris(2-aminoethyl)amine and tetraethylenepentamine. Interestingly, a very different trend was observed when considering the Au/N atomic ratio. Indeed, the highest value (15.5) was obtained for the TRIS-functionalized monolith while the AEP- and TETRA-functionalized monoliths exhibited the lowest values (in the range 6-8). These results clearly highlight the crucial role of the nature of the amine group, primary amine *vs.* secondary amine, over the nitrogen/amine content. Indeed, it is noteworthy that the nitrogen-rich AEP- and TETRA-functionalized monoliths, containing only or mainly secondary amines for AEP- and TETRA-functionalized monoliths, respectively, provide a low efficiency for the amine-driven immobilization of gold nanoparticles. In contrast, the TRIS-functionalized monolith bearing two primary amine groups per grafted ligand exhibits the highest efficiency in terms of nitrogen-mediated gold capture. An intermediate behaviour is observed for the ethylene diamine-grafted monolith.

a.



b.

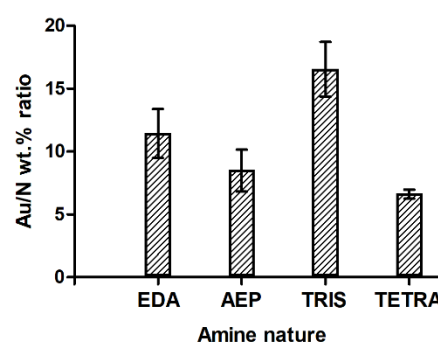


Figure 2. a) Nitrogen over carbon and b) gold over nitrogen atomic ratios as determined by EDX for hybrid EDA-, AEP-, TRIS- and TETRA-functionalized monoliths with supported gold nanoparticles.

Influence of the nature of the grafted ligand was also noticed by SEM observations. Indeed, the images recorded for the functionalized hybrid monoliths demonstrated the strong influence of the immobilized ethylene diamine-based ligands over the AuNP morphology and size (Figure S3 & 3).

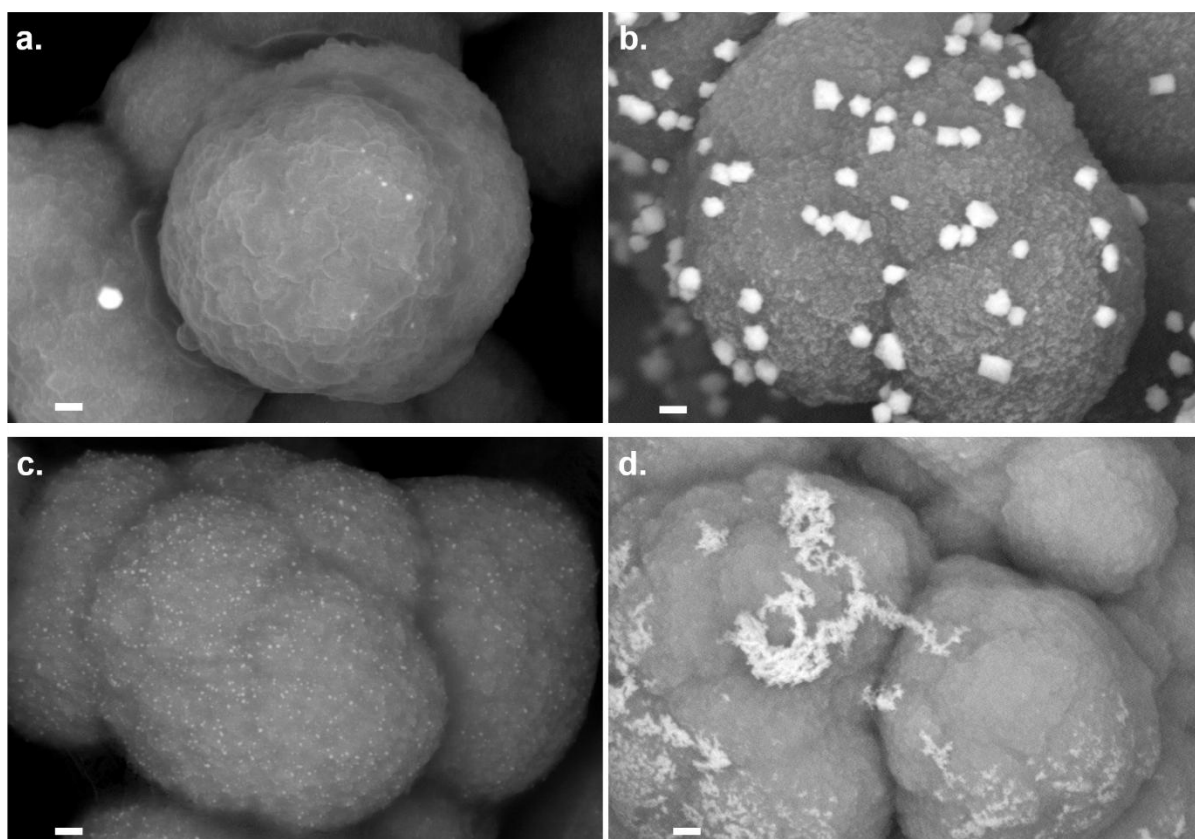


Figure 3. Magnification of SEM pictures of gold nanoparticles immobilized through the *in-situ* strategy onto a) EDA-, b) AEP-, c) TRIS- and d) TETRA-functionalized Poly(NAS-*co*-EGDMA) monoliths. Scale bar = 100 nm.

Both size, shape, surface density and dispersion of *in-situ* synthesized AuNPs at the surface of functionalized monoliths was varied depending on the nature, primary *vs.* secondary, of the amine group (Table S2). The grafting of TRIS on the surface of Poly(NAS-*co*-EGDMA) monolith allowed for obtaining low-sized spherical nanoparticles with diameters below 20 nm (9 ± 3 nm), barely distinguishable by SEM, and homogeneously and densely distributed over the monoliths' surface (Figure 3 c). Larger gold nanoparticles with size in the 60 - 200 nm range and different shapes were observed on the surface of the EDA- and AEP-functionalized monolith (Table S2). These nanostructures are sparsely but homogeneously

present at the monolith surface. Based on the EDX results, it is assumed that low-sized gold nanoparticle that cannot be observed through SEM analysis are also present at the surface of such monoliths. A very different morphology was observed for the TETRA-functionalized monolith for which a rather inhomogeneous disparity of the nanoparticles diameter along with the presence of many aggregates were obtained.

3.3. Supported catalysis associated with reduction of nitroarenes

AuNPs are prone to act as nanocatalysts for the reduction of nitroarene compounds in the presence of sodium borohydride.[11] To this purpose, different solution of nitroarenes (namely *o*-nitrophenol, *p*-nitroaniline and 4-chloro-7-nitrobenzofurazan, see Figure 4) along with NaBH₄ in water were freshly prepared and injected through the loop of an HPLC pump to a 10 cm long EDA-, AEP-, TRIS- or TETRA-functionalized NAS-based capillary containing *in-situ* generated AuNPs at a flow rate of 3 $\mu\text{L}\cdot\text{min}^{-1}$.



Figure 4. Chemical structure of the different nitro-containing aromatic compounds reduced by in-capillary flow-through AuNP-catalyzed reaction in the presence of an excess of NaBH₄.

Solutions harvested at the outlet of the four different capillaries were analyzed by off-line UV-Visible spectrophotometry (**Figure 5**). The four hybrid monoliths did not exhibit significant differences in their catalytic efficiency and complete conversion was obtained for *o*-nitrophenol and *p*-nitroaniline. This result was rather in contradiction with previous contributions that hypothesized that the smaller the nanoparticles, the higher the yield. Considering the catalytic reduction of 4-chloro-7-nitrobenzofurazan, a not commonly studied compound, one may conclude that the lowest yield of conversion (32%) was obtained for the TETRA-functionalized monolith exhibiting gold nanoparticle aggregation (Table 1).

Table 1. Yields obtained upon flow-through reduction of the different nitroaromatic compounds in the hybrid microcolumns depending on the grafted ethylene diamine derivative.

Ligand immobilized	Yield (%)		
		<i>o</i> -nitro-phenol	<i>p</i> -nitro-aniline

EDA	~100	~100	73
AEP	~100	~100	67
TRIS	~100	~100	76
TETRA	~100	~100	32

In contrast, the highest yields of conversion were obtained for the EDA- (73%) and TRIS-functionalized (76%) monoliths for which the gold nanoparticles are chelated by primary amines. Decreasing the flow rate enabled increasing the yield of conversion and complete catalytic reduction of 4-chloro-7-nitrobenzofurazan was obtained for a flow rate of $1\mu\text{L}\cdot\text{min}^{-1}$.

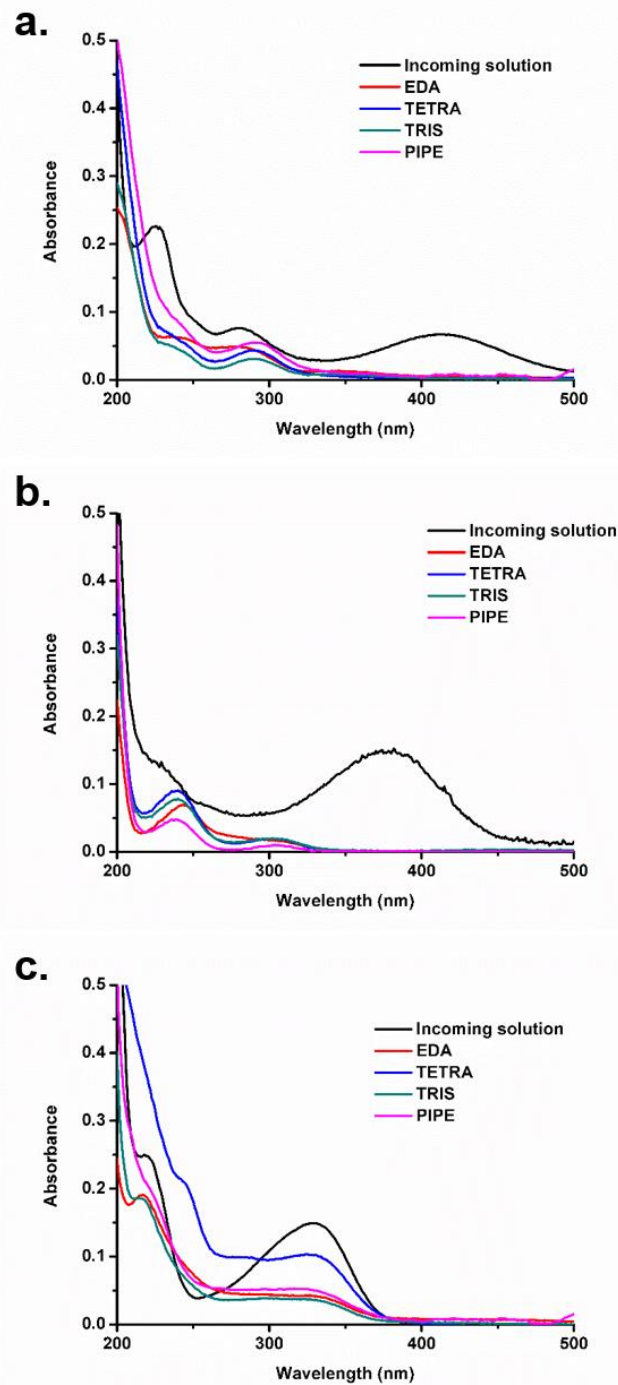


Figure 5. UV-visible absorption spectra recorded in the 200–550 nm wavelength range for solutions of a) *o*-nitrophenol, b) *p*-nitroaniline and c) 4-chloro-7-nitrobenzofurazan in ethanol supplemented with an excess of NaBH_4 before (black trace) and after percolation through EDA- (red trace), AEP- (pink trace), TRIS- (green trace) or TETRA- (blue trace) functionalized monolithic capillaries with supported gold nanoparticles.

4. Conclusions

The different amine ligands deriving from ethylenediamine exposed at the pore surface of in-capillary monoliths play a key role regarding the subsequent immobilization of

gold nanoparticles on such macroporous materials. Even if the gold content immobilized at the interface of monoliths is similar, SEM micrographs clearly demonstrate that the shape and the diameter of adsorbed gold nanoparticles depend on the grafted ligand, while the homogeneity of the dispersion of nanogold and/or the presence of aggregates at the pore surface is also impacted by the nature of the ligand grafted on such porous materials. Finally, such differences in the nanogold shape, diameter and dispersion homogeneity have a significative influence regarding the catalytic reduction of a variety of nitroarenes. Unexpectedly, best nitroarene reduction yield are obtained with monoliths on which are immobilized AuNPs with the largest size (*i.e.* EDA and AEP).

This investigation paves the way to the development of tailored amine-functionalized monoliths for the supported heterogeneous catalysis of a wide array of organic reactions.

Acknowledgements

This manuscript is in honor of the 50-year anniversary of the French Polymer Group (Groupe Français d'études et d'applications des Polymères - GFP). Financial support from CNRS and UPEC is gratefully acknowledged. The authors are indebted to UPEC for providing R. P. with a PhD grant.

References

1. Liu, Y.; Guerrouache, M.; Kebe, S. I.; Carbonnier, B.; Le Droumaguet, B., Gold Nanoparticle-Supported Histamine-Grafted Monolithic Capillaries as Efficient Microreactors for Flow through Reduction of Nitro-Containing Compounds. *Journal of Materials Chemistry A* **2017**.
2. Poupert, R.; El Houda, D. N.; Chellapermal, D.; Guerrouache, M.; Carbonnier, B.; Le Droumaguet, B., Novel in-capillary polymeric monoliths arising from glycerol carbonate methacrylate for flow-through catalytic and chromatographic applications. *Rsc Advances* **2016**, *6* (17), 13614-13617.
3. Poupert, R.; Le Droumaguet, B.; Guerrouache, M.; Carbonnier, B., Copper nanoparticles supported on permeable monolith with carboxylic acid surface functionality: Stability and catalytic properties under reductive conditions. *Materials Chemistry and Physics* **2015**, *163*, 446-452.
4. Floris, P.; Twamley, B.; Nesterenko, P. N.; Paull, B.; Connolly, D., Agglomerated polymer monoliths with bimetallic nano-particles as flow-through micro-reactors. *Microchimica Acta* **2012**, *179* (1-2), 149-156.
5. Floris, P.; Twamley, B.; Nesterenko, P. N.; Paull, B.; Connolly, D., Fabrication and characterisation of gold nano-particle modified polymer monoliths for flow-through catalytic reactions and their application in the reduction of hexacyanoferrate. *Microchimica Acta* **2014**, *181* (1-2), 249-256.
6. Poupert, R.; Grande, D.; Carbonnier, B.; Le Droumaguet, B., Porous polymers and metallic nanoparticles: A hybrid wedding as a robust method toward efficient supported catalytic systems. *Progress in Polymer Science* **2019**, *96*, 21-42.
7. Svec, F.; Frechet, J. M. J., Continuous rods of macroporous polymer as high-performance liquid chromatography separation media. *Analytical Chemistry* **1992**, *64* (7), 820-822.
8. Svec, F., Quest for organic polymer-based monolithic columns affording enhanced efficiency in high performance liquid chromatography separations of small molecules in isocratic mode. *Journal of Chromatography A* **2012**, *1228*, 250-262.
9. Féral-Martin, C.; Birot, M.; Deleuze, H.; Desforges, A.; Backov, R., Integrative chemistry toward the first spontaneous generation of gold nanoparticles within macrocellular polyHIPE supports (Au@polyHIPE) and their application to eosin reduction. *Reactive and Functional Polymers* **2007**, *67* (10), 1072-1082.
10. Harish, S.; Mathiyarasu, J.; Phani, K. L. N.; Yegnaraman, V., Synthesis of Conducting Polymer Supported Pd Nanoparticles in Aqueous Medium and Catalytic Activity Towards 4-Nitrophenol Reduction. *Catalysis Letters* **2009**, *128* (1-2), 197-202.
11. Kuroda, K.; Ishida, T.; Haruta, M., Reduction of 4-nitrophenol to 4-aminophenol over Au nanoparticles deposited on PMMA. *Journal of Molecular Catalysis A: Chemical* **2009**, *298* (1-2), 7-11.
12. Cassol, C. C.; Umpierre, A. P.; Machado, G.; Wolke, S. I.; Dupont, J., The Role of Pd Nanoparticles in Ionic Liquid in the Heck Reaction. *Journal of the American Chemical Society* **2005**, *127* (10), 3298-3299.
13. Mandal, S.; Roy, D.; Chaudhari, R. V.; Sastry, M., Pt and Pd Nanoparticles Immobilized on Amine-Functionalized Zeolite: Excellent Catalysts for Hydrogenation and Heck Reactions. *Chemistry of Materials* **2004**, *16* (19), 3714-3724.
14. Venkatesan, P.; Santhanalakshmi, J., Designed Synthesis of Au/Ag/Pd Trimetallic Nanoparticle-Based Catalysts for Sonogashira Coupling Reactions. *Langmuir* **2010**, *26* (14), 12225-12229.

15. Han, J.; Liu, Y.; Guo, R., Facile Synthesis of Highly Stable Gold Nanoparticles and Their Unexpected Excellent Catalytic Activity for Suzuki–Miyaura Cross-Coupling Reaction in Water. *Journal of the American Chemical Society* **2009**, *131* (6), 2060-2061.
16. Gallon, B. J.; Kojima, R. W.; Kaner, R. B.; Diaconescu, P. L., Palladium Nanoparticles Supported on Polyaniline Nanofibers as a Semi-Heterogeneous Catalyst in Water. *Angewandte Chemie International Edition* **2007**, *46* (38), 7251-7254.
17. Jiang, Z.-J.; Liu, C.-Y.; Sun, L.-W., Catalytic Properties of Silver Nanoparticles Supported on Silica Spheres. *The Journal of Physical Chemistry B* **2005**, *109* (5), 1730-1735.
18. Ma, Z.; Overbury, S. H.; Dai, S., Gold Nanoparticles as Chemical Catalysts. In *Encyclopedia of Inorganic Chemistry*, John Wiley & Sons, Ltd: 2006.
19. Le Droumaguet, B.; Poupart, R.; Grande, D., “Clickable” thiol-functionalized nanoporous polymers: from their synthesis to further adsorption of gold nanoparticles and subsequent use as efficient catalytic supports. *Polymer Chemistry* **2015**, *6* (47), 8105-8111.
20. Poupart, R.; Benlahoues, A.; Le Droumaguet, B.; Grande, D., Porous Gold Nanoparticle-Decorated Nanoreactors Prepared from Smartly Designed Functional Polystyrene-block-Poly(d,l-Lactide) Diblock Copolymers: Toward Efficient Systems for Catalytic Cascade Reaction Processes. *ACS Applied Materials & Interfaces* **2017**, *9* (37), 31279-31290.
21. Poupart, R.; Le Droumaguet, B.; Guerrouache, M.; Grande, D.; Carbonnier, B., Gold nanoparticles immobilized on porous monoliths obtained from disulfide-based dimethacrylate: Application to supported catalysis. *Polymer* **2017**, *126*, 455-462.
22. Ly, H. B.; Poupart, R.; Carbonnier, B.; Monchiet, V.; Le Droumaguet, B.; Grande, D., Versatile functionalization platform of biporous poly(2-hydroxyethyl methacrylate)-based materials: Application in heterogeneous supported catalysis. *Reactive & Functional Polymers* **2017**, *121*, 91-100.
23. Khalil, A. M.; Georgiadou, V.; Guerrouache, M.; Mahouche-Chergui, S.; Dendrinou-Samara, C.; Chehimi, M. M.; Carbonnier, B., Gold-decorated polymeric monoliths: In-situ vs ex-situ immobilization strategies and flow through catalytic applications towards nitrophenols reduction. *Polymer* **2015**, *77*, 218-226.
24. Cao, Q.; Xu, Y.; Liu, F.; Svec, F.; Fréchet, J. M. J., Polymer Monoliths with Exchangeable Chemistries: Use of Gold Nanoparticles As Intermediate Ligands for Capillary Columns with Varying Surface Functionalities. *Analytical Chemistry* **2010**, *82* (17), 7416-7421.
25. Xu, Y.; Cao, Q.; Svec, F.; Fréchet, J. M. J., Porous Polymer Monolithic Column with Surface-Bound Gold Nanoparticles for the Capture and Separation of Cysteine-Containing Peptides. *Analytical Chemistry* **2010**, *82* (8), 3352-3358.
26. Guerrouache, M.; Mahouche-Chergui, S.; Chehimi, M. M.; Carbonnier, B., Site-specific immobilisation of gold nanoparticles on a porous monolith surface by using a thiol–yne click photopatterning approach. *Chemical Communications* **2012**, *48* (60), 7486-7488.
27. Westcott, S. L.; Oldenburg, S. J.; Lee, T. R.; Halas, N. J., Formation and Adsorption of Clusters of Gold Nanoparticles onto Functionalized Silica Nanoparticle Surfaces. *Langmuir* **1998**, *14* (19), 5396-5401.
28. Nguyen, D. T.; Kim, D.-J.; So, M. G.; Kim, K.-S., Experimental measurements of gold nanoparticle nucleation and growth by citrate reduction of H₂AuCl₄. *Advanced Powder Technology* **2010**, *21* (2), 111-118.
29. Polte, J.; Erler, R.; Thünemann, A. F.; Sokolov, S.; Ahner, T. T.; Rademann, K.; Emmerling, F.; Kraehnert, R., Nucleation and Growth of Gold Nanoparticles Studied via in situ Small Angle X-ray Scattering at Millisecond Time Resolution. *ACS Nano* **2010**, *4* (2), 1076-1082.

30. Spano, F.; Massaro, A.; Blasi, L.; Malerba, M.; Cingolani, R.; Athanassiou, A., In Situ Formation and Size Control of Gold Nanoparticles into Chitosan for Nanocomposite Surfaces with Tailored Wettability. *Langmuir* **2012**, *28* (8), 3911-3917.
31. Mehrabanian, M.; Fragouli, D.; Morselli, D.; Scarpellini, A.; Anyfantis, G. C.; Athanassiou, A., Laser-induced localized formation of silver nanoparticles on chitosan films: study on particles size and density variation. *Materials Research Express* **2015**, *2* (10), 105014.
32. Mehrabanian, M.; Morselli, D.; Caputo, G.; Scarpellini, A.; Palazon, F.; Athanassiou, A.; Fragouli, D., Laser-induced in situ synthesis of Pd and Pt nanoparticles on polymer films. *Applied Physics A* **2016**, *122* (12), 1075.
33. Zhang, Q.; Xu, J.-J.; Liu, Y.; Chen, H.-Y., In-situ synthesis of poly(dimethylsiloxane)-gold nanoparticles composite films and its application in microfluidic systems. *Lab on a Chip* **2008**, *8* (2), 352-357.
34. SadAbadi, H.; Badilescu, S.; Packirisamy, M.; Wüthrich, R., Integration of gold nanoparticles in PDMS microfluidics for lab-on-a-chip plasmonic biosensing of growth hormones. *Biosensors and Bioelectronics* **2013**, *44*, 77-84.
35. Morselli, D.; Campagnolo, L.; Prato, M.; Papadopoulou, E. L.; Scarpellini, A.; Athanassiou, A.; Fragouli, D., Ceria/Gold Nanoparticles in Situ Synthesized on Polymeric Membranes with Enhanced Photocatalytic and Radical Scavenging Activity. *ACS Applied Nano Materials* **2018**, *1* (10), 5601-5611.
36. Guerrouache, M.; Mahouche-Chergui, S.; Chehimi, M. M.; Carbonnier, B., Site-specific immobilisation of gold nanoparticles on a porous monolith surface by using a thiol-yne click photopatterning approach. *Chemical Communications* **2012**, *48* (60), 7486-7488.
37. Poupard, R.; Le Droumaguet, B.; Guerrouache, M.; Grande, D.; Carbonnier, B., Gold nanoparticles immobilized on porous monoliths obtained from disulfide-based dimethacrylate: Application to supported catalysis. *Polymer* **2017**.
38. Turkevich, J.; Stevenson, P. C.; Hillier, J., A study of the nucleation and growth processes in the synthesis of colloidal gold. *Discussions of the Faraday Society* **1951**, *11* (0), 55-75.
39. Kimling, J.; Maier, M.; Okenve, B.; Kotaidis, V.; Ballot, H.; Plech, A., Turkevich Method for Gold Nanoparticle Synthesis Revisited. *The Journal of Physical Chemistry B* **2006**, *110* (32), 15700-15707.
40. Carbonnier, B.; Guerrouache, M.; Denoyel, R.; Millot, M. C., CEC separation of aromatic compounds and proteins on hexylamine-functionalized N-acryloxysuccinimide monoliths. *Journal of Separation Science* **2007**, *30* (17), 3000-3010.
41. Dao, T. T. H.; Guerrouache, M.; Carbonnier, B., Thiol-yne Click Adamantane Monolithic Stationary Phase for Capillary Electrochromatography. *Chinese Journal of Chemistry* **2012**, *30* (10), 2281-2284.
42. Guerrouache, M.; Carbonnier, B.; Vidal-Madjar, C.; Millot, M. C., In situ functionalization of N-acryloxysuccinimide-based monolith for reversed-phase electrochromatography. *Journal of Chromatography A* **2007**, *1149* (2), 368-376.
43. Guerrouache, M.; Millot, M. C.; Carbonnier, B., Functionalization of Macroporous Organic Polymer Monolith Based on Succinimide Ester Reactivity for Chiral Capillary Chromatography: A Cyclodextrin Click Approach. *Macromolecular Rapid Communications* **2009**, *30* (2), 109-113.
44. Guerrouache, M.; Millot, M. C.; Carbonnier, B., Capillary columns for reversed-phase CEC prepared via surface functionalization of polymer monolith with aromatic selectors. *Journal of Separation Science* **2011**, *34* (16-17), 2271-2278.

45. Tijnelyte, I.; Babinot, J.; Guerrouache, M.; Valincius, G.; Carbonnier, B., Hydrophilic monolith with ethylene glycol-based grafts prepared via surface confined thiol-ene click photoaddition. *Polymer* **2012**, *53* (1), 29-36.
46. Zhu, H.; Du, M.; Zou, M.; Xu, C.; Li, N.; Fu, Y., Facile and green synthesis of well-dispersed Au nanoparticles in PAN nanofibers by tea polyphenols. *Journal of Materials Chemistry* **2012**, *22* (18), 9301-9307.